# Design of retrofit devices using CFD, validated with wind tunnel tests

**Marion C. James***, **Stephen R. Turnock, Dominic A. Hudson**

Fluid-Structure Interactions Research Group; University of Southampton, Southampton, UK. SO17 1BJ

## 1 Introduction

With the increase in fuel prices and growing pressure on the marine industry to reduce greenhouse gas emissions, there is a demand for ships in operation to develop novel ways to reduce both their fuel consumption and emissions. In 2009, the International Maritime Organisation (IMO) published methods on how both new and existing ships would be assessed on their emissions in the future via the Energy Efficiency Design Index (EEDI) and Energy Efficiency Operations Indicator (EEOI) respectively. As a conceptual idea, these indices may be expressed as the ratio between $CO_2$ emissions and the amount of transport work done for a ship.

This paper presents how the efficiency of an existing tanker hull form could be increased by 10% with the use of cost-effective retro-fit solutions. A method, involving CFD simulations performed using OpenFOAM® and validated with wind tunnel tests, is explained. An in-house code, based on the Blade-Element Momentum Theory (BEMT), is used to provide some propeller characteristics: efficiency, torque and thrust coefficients. Although, the efficiency output from the BEMT code is not the propulsive coefficient, $\eta_D$, the different appendage configurations may still be directly compared using this efficiency, denoted $\eta_{BEMT}$ throughout this paper.

## 2 Wind Tunnel Testing

### 2.1 Benefits

Experiments were carried out in the Mitchell Wind Tunnel at the University of Southampton. These experiments are used to validate the CFD simulations and allow for an analysis of the existing naked hull form to be performed. The study of the naked hull is used as a benchmark to illustrate any flow changes observed in future investigations.

Using wind tunnel tests offers two main advantages. First, the model scale factor can be smaller when compared to towing tank tests,resulting in a Reynolds number high enough to model a steady turbulent flow as experienced by the full scale ship. Furthermore, in a wind tunnel, wake pressure measurements are not affected by free surface effects (wave pattern).

### 2.2 Model Dimensioning

In order to accurately model the effect of retro-fit devices on the flow around the hull, it is important to ensure that the turbulent flow condition around the full scale ship is replicated at model scale. The onset of turbulent flow will occur, even on smooth bodies, when the Reynolds number exceeds $0.5 \times 10^6$ (Molland and Turnock 2007).

The Reynolds number of the full scale ship is calculated to be $1.187 \times 10^9$, confirming the need for turbulent flow around the experimental model. The 3.5m x 2.1m closed return Mitchell Wind Tunnel was used to its limit with a working section accepting models of upto 4m long and with a wind speed of 30m/s. The maximum achievable Reynolds number is $7.648 \times 10^6$.

Since only the stern flow is of interest in this investigation, the parallel mid-body is truncated as shown in Figure 1. This modification is made providing the flow without the parallel middle body is sufficiently similar to that required. It is in the assessment of this that CFD provides considerable use. A 4m model with a much smaller scale factor may thus be tested, reducing the magnitudes of the experimental and scaling errors.

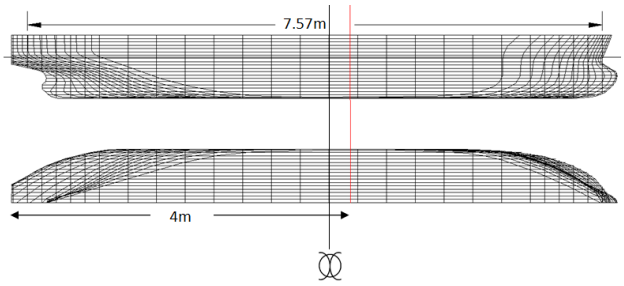


Figure 1: Truncated model length

The scale factor is calculated based on the assumption that at the propeller plane, the boundary layer thickness, $\delta$ (viscous wake), is approximately half of the propeller diameter. The boundary layer thickness is estimated, for the wrap around length of the 4m model, using the 1/7 power-law velocity distribution displayed in Equation 2.1 below:

$$\frac{\delta}{x} = 0.370 Re_x^{\frac{-1}{7}} \tag{2.1}$$

From these calculations the diameter of the propeller for the model is known and hence a scale of 1/23 is selected. For a 1/23 scale model, a blockage of 9.25% is created but still within the 10% limit where corrections may be applied. The dimensions of the wind tunnel model are summarised in Table 1.

Table 1: Wind tunnel model dimensions

| | | Ship | Model |
|---|---|---|---|
| Length, Over All | (m) | 183.88 | 4.00 |
| Breadth | (m) | 32.2 | 1.40 |
| Draught | (m) | 12.416 | 0.54 |
| $C_B$ | | 0.8 | - |
| Propeller Diameter | (m) | 6.00 | 0.26 |
| $\delta$ (at propeller plane) | (m) | 1.40 | 0.14 |
| % Blockage | | | 9.25 |

*corresponding author's e-mail: mcj1g08@soton.ac.uk

## 2.3 Method of Wind Tunnel Testing

The wind tunnel experiments are aimed at recording pressures in the wake field and at the propeller plane of the truncated model. A traverse rig is used to move a Pitôt rake to the required locations. In addition, pressure tappings are employed to monitor that the flow reattached to the model at the stern despite the truncated bow. A schematic diagram of the set-up of the test may be seen in Figure 2.

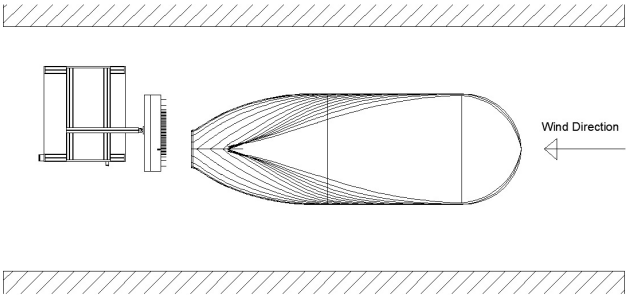


Figure 2: Wind tunnel test set-up with the wake traverse rig shown downstream of the model.

To qualitatively assess the flow pattern in the wind tunnel, tufts and an oil based paint are used. A matrix of x by y measurements is made at the desired plane using an automated traverse. The recorded pressures in Pascals are converted into velocities using the simplified form of the incompressible Bernoulli's equation. For each test, the velocities are non-dimensionalised with the free stream velocity, $U$. Velocity contour plots are then generated at different planes at the stern.

The different appendages are compared based on the propeller efficiency. The blade-element momentum theory (Phillips et al, 2009) requires the wake fraction at specific locations int the propeller plane. As a result, a wake analysis is conducted. The Taylor wake fraction $w_T$ is a measure of how the hull influences the velocity of the flow in the propeller region, and it may be expressed as:

$$w_T = 1 - \frac{u}{U} \tag{2.2}$$

# 3 Numerical Set-Up: Computational Fluid Dynamics

## 3.1 Pre-processing

In order to effectively simulate the wind tunnel experiments and to investigate the design of the retrofit devices, the initial conditions of the CFD simulations are carefully chosen.

The domain size is based on the wind tunnel dimensions, such that the same blockage effect encountered by the model in the experiments is computationally modelled. However, due to the complexity of the wind tunnel, only the working section length is incorporated within the simulation (1.5L upstream and 3L downstream).

The boundary conditions applied to the domain and geometry are chosen in a similar manner to the domain size. The inlet and outlet boundary field types are defined as a fixed velocity inlet/outlet respectively (U = 30m/s). The hull form is defined as a non-slip wall, and the upper and side walls are given a slip condition. The effect of the slip condition is deemed to have a negligible effect on the flow around the model, when compared to the experimental results. The bottom wall is defined as a symmetry wall, as it may be used to simulate the free surface effect within the wind tunnel environment.

The mesh is generated using a hybrid technique, where a structured boundary layer mesh is surrounded by an unstructured domain mesh. Two refinement cylinders located on each bilge keel and one refinement box located at the aft section of the hull form are added. These regions are chosen as key areas to refine the mesh in order to correctly capture the flow around the bilges and the stern. The boundary layer mesh parameters are selected for a $y^+$ value of 30 and a minimum total thickness of 8mm (based on flat plate theory).

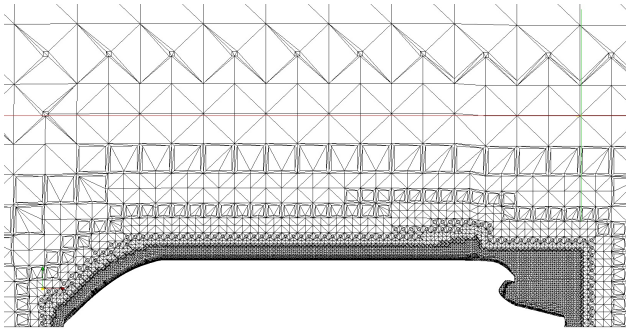

Figure 3: Final mesh along the x-direction

Overall, the quality of the mesh is reasonably good with just over one million elements. The parameters used to define the boundary layer mesh provide a 99.5% extrusion success. Figure 3 shows a smooth growth rate across the domain, allowing accurate interpolation of the field properties between elements. However, the thickness of the inner refinement level should ideally be reduced to limit the element counts without vastly compromising the accuracy of the solution. This could not be completed due to the inability to further refine the inner level with the available computational resources.

## 3.2 Simulation

Being a steady-state problem, the OpenFOAM® solver simpleFoam is chosen to simulate the flow around the hull form (single phase). This solver is based on a Semi-Implicit Method for Pressure-Linked Equation (SIMPLE) and uses a pressure correction. The flow properties are solved until the predefined convergence criteria are met ($10^{-6}$ - Good convergence).

Since this study is based on a RANS simulation, the SIMPLE algorithm requires a turbulence model. The $k-\omega$ SST model is chosen to be the most appropriate.

## 3.3 Verification and Validation Studies

In order to verify CFD simulations, several analyses may be performed: $y^+$ value, domain analysis, mesh dependency study and turbulence model analysis. Initially, the $y^+$ value is checked to ensure compatibility with the chosen

turbulence model, $k-\omega$ SST. As required, $y^+$ lies between 30 and 250.

In addition, a domain analysis is conducted. Since the width and height of the domain are restricted (wind tunnel cross-section), only the effect of the domain length is assessed. The lengths upstream and downstream are increased; but the efficiency differences prove to be negligible.

The next step in the validation process is to undertake a mesh dependency study. The refinement process is completed using a systematic approach. The base size is multiplied by a factor of $2\sqrt{2}$ repetitively until a desired mesh resolution is achieved (greater than 10 million) without modifying the boundary layer mesh. The efficiencies obtained from the BEMT code for each mesh are within the error band of the wind tunnel experiments. This proves that the mesh used has a a sufficient resolution to achieve convergence of the results. Further details of this process and of the experiment may be found in Collison et al, (2012).

# 4 Naked Hull Results and Analysis

The flow pattern is initially analysed using streamlines. To quantify the results, the local axial velocities from CFD are extracted at the propeller plane to form the wake matrix used in the BEMT code. Moreover, velocity components are probed over the entire propeller plane and further aft in the wake field. Using the visualisation tool 'Paraview', contour plots may then be generated allowing a direct comparison with the wind tunnel test results (Section 4.2).

## 4.1 Effects of Truncation

The effect of the truncation is studied based on the radial distribution of the wake obtained from the CFD simulations. The radial wake fraction may be expressed as:

$$w_T{}' = \frac{1}{2\pi}\int_0^{2\pi} w_T{}'' \, d\theta \qquad (4.1)$$

A comparison between the wind tunnel model (truncated L=4m) and the non-truncated model (L=8m) for identical Reynolds number is undertaken. In addition, a simulation of the non-truncated model with a matching Reynolds number to the full scale ship is completed.

Table 2 shows that the effect of truncation on the flow field is negligible. However, a model scale simulation where the Reynolds number is matched to the full scale ship still induces scaling errors, as the boundary layer thickness does not vary linearly with Reynolds number. The use of oversized devices is therefore required to counteract this effect.

Table 2: Effect of truncation: nominal mean wake

| | $w_T$ |
|---|---|
| **Truncated model - U = 30m/s** | 0.3987 |
| **Non-truncated model - U = 15m/s** | 0.4386 |
| **Non-truncated model - U = 2186m/s** | 0.2773 |

As well as affecting the boundary layer thickness, truncation of the model is likely to affect the flow separation around the model. Similarity of the flow around the truncated model and the full size ship is essential to ensure the validity of the study. Although a certain amount of separation ahead of the point where the devices are to be fitted is tolerable, it is important that the flow reattaches by the time the vanes are reached.

Separation (areas of lower pressure, shown in blue in Figure 4) does occur just aft of the truncated bow but only for a small area before the flow reattaches. Indeed, a slowly increasing pressure with distance towards the stern verifies that the flow is being affected by the presence of the curved hull, suggesting it is attached to the hull. Figure 4 confirms the suitability of using a truncated model. As a validation, pressure tappings are placed on the hull and a similar trend as the CFD predictions is obtained.


Figure 4: Pressure distribution on hull as predicted by CFD

## 4.2 Flow and Wake Fields

The flow pattern is identified using streamlines in CFD and an attempt is made to validate the CFD results in the wind tunnel using oil based paint and tufts, as shown in Figures 5 and 6.

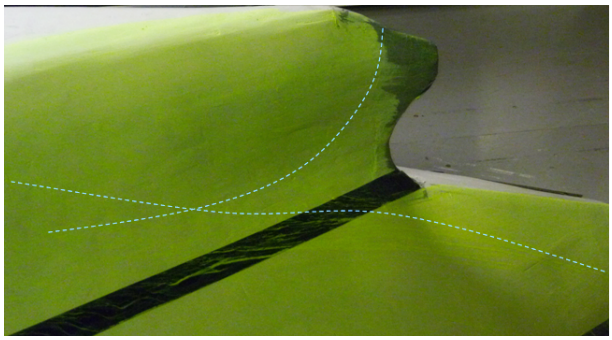

Figure 5: Flow streamlines on the wind tunnel model captured using paraffin oil. Lines are added to highlight different zones.

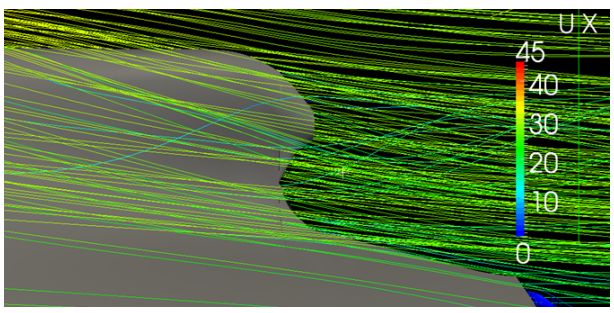


Figure 6: Flow streamlines generated by CFD

A clear similarity between the flow patterns may be observed, suggesting that the flow is diverted away from the propeller plane. Indeed, this first impression may be confirmed upon examination of the contour plots shown in Figure 7. The propeller operates in the region where the flow is slowest, whereas for increased efficiency, it is desirable for the flow into the propeller to have a higher velocity. The figures also confirm that the CFD and wind tunnel wake plots are similar, although the mid-wake obtained in the wind tunnel does seem to be wider and higher than that predicted by CFD. Furthermore, the CFD does not seem to predict the small gradual changes in velocity which can be seen in the experimental wake both in the Y direction (at the propeller plane) and in the Z direction (at the mid-wake).

These differences are likely to explain the discrepancies in efficiency values shown in Table 3. Indeed, when operating in the CFD generated wake, a much greater proportion of the propeller blade is located in the lighter grey region of faster flow, whereas when operating in the experimental wake, the propeller operates in a region of slower flow which gradually increases to the velocity predicted by CFD.

Considering the likely sources of experimental error, combined with the percentage tolerances of the CFD, a difference in efficiency of just over 9% is judged to be acceptable when comparing predictions obtained from computational and experimental methods. This, together with the similar general trends obtained both in wake and hull flow fields, suggests that the CFD simulation provides a reasonable prediction of the wind tunnel results. The CFD simulation may therefore be used to analyse the effect of various devices on the wake field and propeller efficiency.

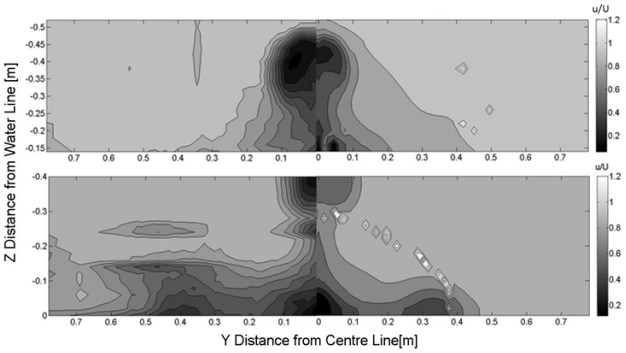


Figure 7: Propeller plane (top) and mid-wake (bottom) contour plots of wind tunnel test 1 (left) and CFD (right)

Table 3: Naked hull results - comparisons of wind tunnel efficiencies against CFD predictions. Test 1 was the initial wind tunnel test session and Test 2 the final refined test process.

| | $K_T$ | $K_Q$ | $\eta_{BEMT}$ | $\Delta\,\eta_{BEMT}$ (%) |
|---|---|---|---|---|
| **CFD** | 0.1920 | 0.0229 | 0.6821 | - |
| **Test 1** | 0.1167 | 0.0153 | 0.6188 | 9.28 |
| **Test 2** | 0.1055 | 0.0146 | 0.7033 | -3.11 |

# 5 Investigation of Devices

## 5.1 CFD Analysis

Based on the initial study of the flow pattern around the naked hull and the research on current retro-fit devices, two main types of devices are retained: vortex generating fins and flow channelling ducts. Since the flow appears to be diverging away from the propeller plane, it is decided to position a vortex generator upstream (see Section 4) to redirect the flow with an increased velocity. Vanes with varying parameters of location, angle and shape are designed and tested in CFD to analyse their effects on the flow field. Moreover, two types of duct are studied: Mewis and Wake Equalising Ducts (WED). The duct design is based on Mewis (2009) and a NACA 0006 section is assumed. Different ratios between inlet and outlet diameter are tested. The devices' dimensions are clearly too large to be realistically fitted onto a ship, but are for research purpose only.

Table 4: Comparison of potential retro-fit devices

| | $K_T$ | $K_Q$ | $\eta_{BEMT}$ | $w_T$ |
|---|---|---|---|---|
| **CFD naked hull** | 0.1920 | 0.0229 | 0.6821 | 0.3987 |
| **Test 1** | 0.1167 | 0.0153 | 0.6188 | - |
| **Vane** | 0.1879 | 0.0225 | 0.6892 | 0.3854 |
| **Duct** | 0.2063 | 0.0245 | 0.6919 | 0.4588 |
| **WED** | 0.2032 | 0.0241 | 0.6501 | 0.4404 |

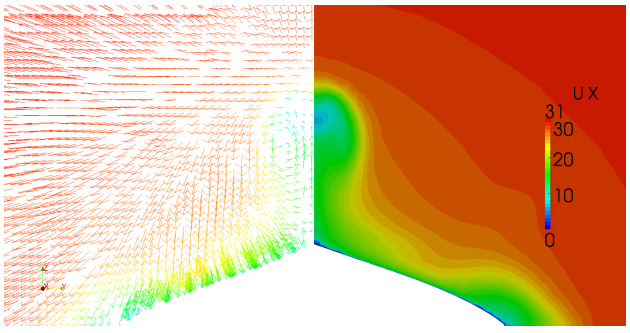


Figure 8: Naked hull wake at propeller plane: velocity vectors and contour plot

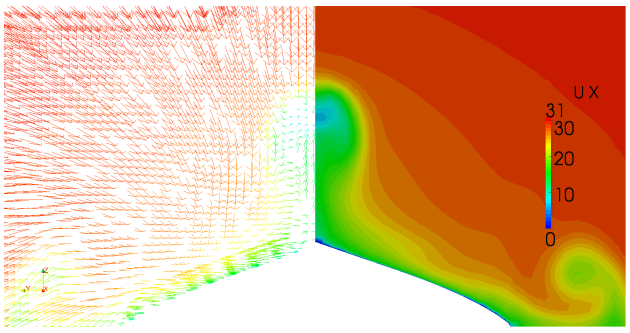


Figure 9: Effect of vane on wake at propeller plane: velocity vectors and contour plot

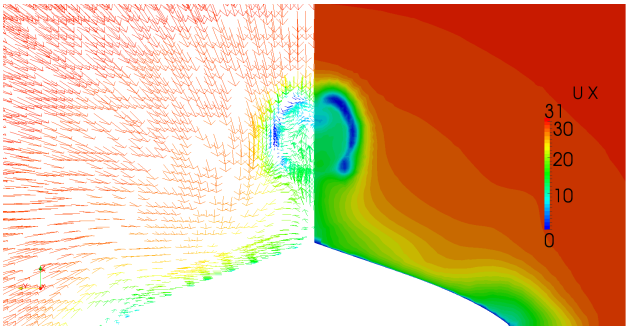


Figure 10: Effect of duct on wake at propeller plane: velocity vectors and contour plot

Qualitative data are extracted from CFD to obtain an initial idea of the impact of adding a device on the flow. Figures 8-10 show contour plots of the axial velocity, where each shade represents a variation of $1m/s$. Table 4 shows a comparison of some devices tested in CFD in preparation of the wind tunnel test 2. Moreover, the nominal wake is calculated from the local wake matrix derived at the propeller plane.

A vane is first tested to obtain an initial estimate of its influence on the flow field. When comparing the velocity plots for the naked hull and with device (Figures 8-9), it may be observed that thanks to the addition of the vane, the flow speed increases at top dead centre. Out of all the vane configuration tested, the best gain in efficiency is found to be 1%. As a result, this vane configuration is suggested to be used as an initial set-up for the wind tunnel test 2. However, since the vane is located too close to the floor the tip vortex and associated flow are reflected. This phenomenon may improve the propeller flow field, hence the increase in efficiency. The introduction of a free-surface in CFD would eradicate this unrealistic flow behaviour.

The initial duct design is modified to an inlet-outlet diameter ratio of 1.3 in order to increase the flow speed into the propeller plane (Figure 10- 'Bernoulli Effect'). This gives an increase of 1.42% in efficiency. Due to the time and manufacturing constraints, it was decided to focus on the development of further vane designs in the wind tunnel; while a duct is tested later on in the towing tank. The attempt of testing a wake equalising duct in order to create a more uniform flow into the propeller plane is not as successful and it shows a slight decrease in efficiency.

Although the addition of retro-fit devices shows overall gains in efficiency, the accuracy of the results still needs to be assessed. The differences in efficiency are minimal (below 2%) and may therefore be considered to be within the 'noise'of CFD.

### 5.2 Wind Tunnel Analysis

Following the CFD analysis, the most promising vane location is tested in the wind tunnel, using variations on the geometry and size of the suggested fin.

The variation in propeller efficiencies across the tested devices is minimal when compared to the naked hull efficiency. However, the greatest recorded change in efficiency is just under 0.02, which equates to a percentage change of around 3%. This is a significant change in efficiency, suggesting the experimental procedure used is successful in measuring the effect of different devices on the wake field.

Despite the high repeatability observed for repeat runs, no general pattern is obtained when relating efficiency to angle of attack and vane size. This suggests many more repeat runs and tests, with a greater range of angles of attack, device sizes and geometries should be undertaken before drawing any conclusions with acceptable confidence.

Although general trends for device design cannot be obtained, the results provide interesting and encouraging evidence that vanes may indeed be effective retro-fit devices. The largest improvement measured is just under 3%.

The result of this slight change in flow around the stern of the hull results in the flow into the propeller being accelerated, as may be seen from Figure 11. This slight acceleration in the flow explains the increase in propeller efficiency obtained.

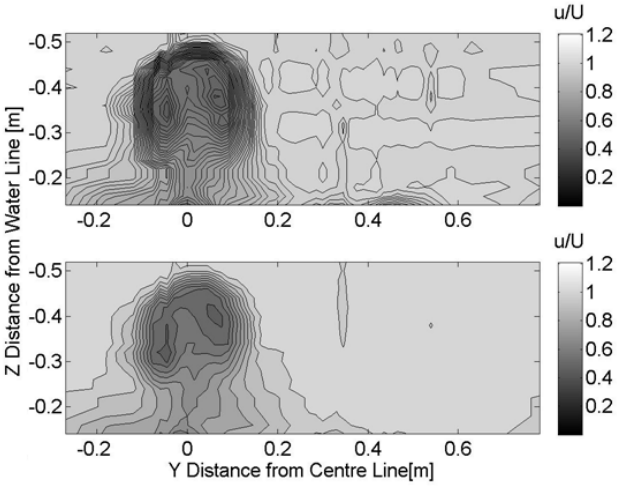


Figure 11: Wake velocities for vane (top) and the naked hull (bottom)

Figure 11 highlights the fact that changes are minimal and very difficult to observe at this scale. Moreover, the magnitude of the changes is such that any experimental error will create a large percentage error in the efficiency value obtained, leading to a high uncertainty value for the obtained results. The considerable increase in efficiency observed on some vanes during this project does however suggest that further work and research in vane development is worthwhile.

## 6 Towing Tank Tests

Further investigations were conducted in the Solent University Towing Tank. A series of naked hull resistance and self-propulsion tests were undertaken using a 1/60 scale geosim ship model. The resistance discrepancy between the naked and appended hull was negligible. Although the normal limits of the towing tank are exceeded (high displacement), definite trends are observed from the variation of device configurations. The decrease in RPM at self-propulsion point after the addition of appendages shows an improvement in performance. The use of the duct, gives a 9.6% gain in the propulsive efficiency. This gain shows the same trend as the results from CFD simulations but these

results are suspected to be unrealistically high. In order to obtain more accurate results, a larger scale towing tank would be required and several load conditions should be tested.

A CFD simulation including a free-surface was completed to increase the physical reality of further investigations of retro-fit devices. However, a high discrepancy between the CFD and towing tank naked hull resistance is observed due to an inaccurate viscous resistance component. An initial verification study is performed in an attempt to understand the source of error, by using different means of obtaining forces and by investigating the effect of the boundary layer mesh. Even though results obtained from this investigation do not determine the source error associated with the viscous resistance, a thorough verification process should be completed.

# 7 Conclusions

Wind tunnel and towing tank experiments are used, in conjunction with open-source computational fluid dynamics modelling, to analyse the wake field changes induced by retro-fit devices. These changes are assessed using the propeller efficiency obtained from blade element momentum theory. A testing procedure is developed, explained in terms of methodology, with justifications for improvements. This procedure successfully detects changes in propeller efficiency at model scale due to devices and thus provides a route to investigate a wide variety of devices.

A cost analysis model was developed to assess the viability of fitting devices on a ship during a routine dry-docking period. Results, based on voyage data provided by the ship operator and European shipyard rates, suggest that a 1% reduction in required delivered power could lead to a payback period of 25 days for devices as simple as a triangular vane. Preliminary results highlight that efficiency gains up to 3% could be obtained with vanes and up to 9% with flow increasing ducts.

# 8 Further Work

To validate the current result and further the initial investigations, testing of devices with a greater range of geometries, angles of attack and locations should be carried out. Moreover, the effect of the devices on the wake in several load conditions should be tested. This analysis would provide a clearer understanding of the relationships between the device parameters and the propeller efficiency gains.

Furthermore, a finite element analysis should be used to calculate the structural loading on each device during service. The feasibility of the chosen retro-fit solution could therefore be determined. Such findings would allow further investigations to determine an optimum retro-fit device for the hull form studied.

# Acknowledgements

The group would like to acknowledge the following people:

The project supervisors, Professor Stephen Turnock and Dr Dominic Hudson, for their continued help and advice during the year.

The project sponsors without whom this project would not have been possible.

All the Ship Science and Faculty staff and research fellows for their support and time throughout the year in towing tank supervision and general availability for consultation and advice.

# Nomenclature

| | | |
|---|---|---|
| $C_B$ | Block coefficient | |
| $K_Q$ | Propeller torque coefficient | |
| $K_T$ | Propeller thrust coefficient | |
| U | Free stream velocity | $[m/s]$ |
| $w_T{}'$ | Taylor wake fraction | |
| $w_T{}''$ | Radial distribution of the wake | |
| $w_T{}''$ | Axial wake component | |
| $y^+$ | Non-dimensional wall distance | |
| $\delta$ | Boundary layer thickness | $[m]$ |
| $\eta_{BEMT}$ | Efficiency from the BEMT code | |
| $\eta_D$ | Propulsive efficiency | |

# References

Collison, R., James, M., Mathieson, S., Rident, C., Scott, C., Unwin, E. (2012) Retro-fit Solutions for Energy Efficient Shipping, Ship Science MEng Group Design Project Report No 41.

IMO (2011) Reduction of GHG Emissions from Ships *MEPC 62/5/17*

Lee, S.J., Kim, H.R., Kim, W.J., Van, S.H. Wind Tunnel Tests on Flow Characteristics of the KRISO 3,600 TEU Containership and 300K VLCC Double-Deck Ship Models. (2003) *Journal of Ship Research*, 47 (1), 24-38

Mewis, F., Guiard, T. (2011) Mewis Duct - New Developments, Solutions and Conclusions *Second International Symposium on Marine Propulsors*

Molland, A.F., Turnock S.R., Hudson D.A. (2011) *Ship Resistance and Propulsion. Practical Estimation of Ship Propulsive Power* New York: Cambridge University Press

Molland, A.F., Turnock S.R.,(2007) *Marine Rudders and Control Surfaces; Principles, Data, Design and Applications* Oxford: Elsevier

Phillips, A.B., Furlong, M.E, Turnock, S.R. (2009) Accurate capture of rudder-propeller interaction using a coupled blade element momentum-RANS approach, 12th Numerical Towing Tank Symposium, Cortona, Italy

Wilcox, D.C. (2006) *Turbulence Modelling for CFD*, 3rd edn., California: Birmingham Press